Comparative Study of Sliding Mode Controller and Incremental Conductance Method to Track Maximum Power Point of Photovoltaic Arrays

Babak Mehdizadeh Gavgani, Department of Electrical Engineering, Seraj University, Tabriz, Iran.

***Abstract*—The output voltage of a solar cell varies due to environmental conditions such as changes in temperature and solar radiation intensity which means that the output power of the photovoltaic (PV) arrays is not constant. The PV output power has a unique maximum power point in every operation conditions. In order to extract the highest efficiency of a solar cell and optimize the PV system performance, it is necessary to track maximum power of a PV cell (MPPT). This paper presents a comparative study of Sliding Mode Controller (SMC) and Incremental Conductance (INC) algorithm to track maximum power point of photovoltaic arrays. Both controllers maximize the output power of the PV system by adjusting the duty cycle of a DC/DC boost converter. The simulations under different environmental variations confirm the stability and the robustness of both controllers however it is shown that the SMC has a better performance and is fast in precise.**

***Index Terms*— DC/DC boost converter, incremental conductance, maximum power point tracking, photovoltaic system, sliding mode controller.**

I. Introduction

It is an undisputable fact that the energy is one of the main vital elements of human life. In recent years the fossil fuels energy resources have decreased significantly and the greenhouse gasses are increasing considerably that cause the global warming effects and natural disasters. These obstacles highlight the necessity for an alternative energy source that is environmentally friendly and economical. Among renewable energy sources (wind, solar, etc.), solar energy is the most popular one which is easily accessible and clean.

The output characteristics of a PV cell highly depend on the environmental changes so the maximum power point (MPP) of the PV system is unique in every insulation and temperature. To optimize the PV system performance, it is important to gain the maximum power from the PV module by stabilizing the PV power at its optimal point (MPP). Vast numbers of MPPT algorithms have been presented these years. The most common strategy is to adjust the duty cycle of a converter according to the output power of the PV module to place the PV system at its maximum power whiles the variations of insulation and temperature can occur at any time [1]- [4]. A look-up table method is proposed in [5] which is based on the parameters and typical curves of the PV module under different situations. Curve-fitting algorithm in [6] models the nonlinear characteristics of a PV by mathematical approximations. The most obvious drawback for these methods is that they need a large memory to store data which increases the economic costs. Another technique that is presented in [7], [8] is open-circuit voltage method. At this algorithm the MPPT unit approximates a linear equation between the PV voltage at MPP (V_{MPP}) and the PV output voltage. The short-circuit current method has the similar principles of the open-circuit voltage algorithm but it uses PV current instead of PV voltage [9], [10]. These algorithms are offline techniques in other words they will not respond acceptable at changeable environmental conditions which means losing power. The techniques that are mostly used to track maximum power point are Perturb and Observe (P&O) and hill-climbing algorithms [11]-[15]. The principle of these two techniques is perturbing the PV voltage (V_{PV}) (by changing the duty cycle of the converter) and observing the P_{PV}. If P_{PV} increases, further adjustments in the duty cycle are tried in the same direction until power no longer increases. Despite of that the implementations of these methods are simple; the output power oscillation problem can be counted as big disadvantage of them. Incremental Conductance method in [16] is a famous MPPT algorithm is based on the fact that the P_{PV} slope is zero at MPP. Sliding mode controller is introduced in [17], [18]. In this method first the sliding surface that determines the optimal states of the system variables (V_{MPP}, I_{MPP}) is defined and then the SMC converges the system controllable states to it (MPPT). Fuzzy Logic Controller (FLC) in [19], [20] does not need any exact model of the PV system and tracks the maximum power properly.

This paper provides a comparative study of sliding mode controller and INC method to track maximum power of the PV module and evaluates their performance through simulation results for different conditions. The paper is organized as follow: The PV cell characteristics are given in Section II. MPPT system modeling is described in section III. Simulation results and conclusion are presented in Section IV and V, respectively.

Submission date: 01 December 2017, Publication date: 31 January 2018.
Corresponding Author: (E-mail: babak.mehdizadeh.gv@gmail.com).

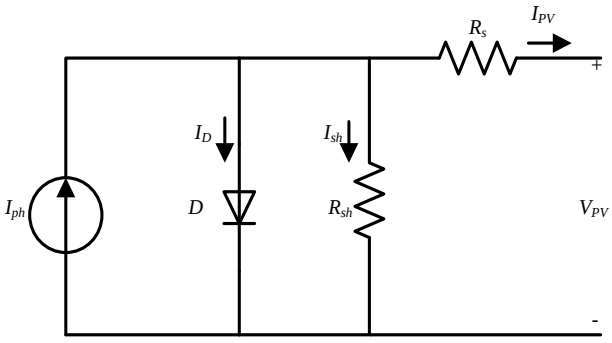

Fig.1. Equivalent circuit model of a PV cell.

II. PV Cell Characteristics

The equivalent circuit model of a PV is shown in Fig.1. It consists of a light-generated current source (I_{ph}), Diode (D), Series and Parallel resistances (R_S, R_{Sh}) [12]:

The equations of the PV module are as follows:

$$I_{ph} = \frac{G}{G_0}\left[I_{scr} + k_i\left(T - T_r\right)\right] \quad (1)$$

$$I_D = I_{rr}\left[\frac{T}{T_r}\right]^3 \cdot \exp\left(\left(\frac{T_r - T}{T_r}\right)\cdot\frac{-qE_g}{kT}\right) \quad (2)$$

$$I_{rr} = \frac{I_{scr}}{\left(\exp\left(\frac{qV_{oc}}{N_s kAT_j}\right) - 1\right)} \quad (3)$$

where, I_{ph} is the light generated current, G and G_0 are solar irradiance and reference solar irradiance, respectively. I_{scr} is the PV short-circuit current at reference condition, T and T_r are the temperature and reference temperature of the solar cell, respectively. E_g denotes the band-gap energy of the solar cell, q is the electron charge, N_s is the number of solar cells in series, k_i is the short-circuit temperature coefficient, and k is the Boltzmann's constant.

In this paper the Siemens photovoltaic module has been used for simulations [18]. The parameters of the module are given in Table I. The PV module is made of 72 cells connected in series.

In Fig.2 ($I_{PV} - V_{PV}$) characteristics of the PV module are plotted for different insulations and temperatures.

TABLEI
PARAMETERS OF THE PV MODULE

Parameter	Value
Ideality factor (A)	1.12
Band-gap energy (E_g)	1.12 V
PV short-circuit current (I_{sc})	3.45 A
Short-circuit temperature coefficient (k_i)	1.7 mA/°C
Number of cells in series (N_S)	72
PV open-circuit voltage (V_{oc})	43.5 V

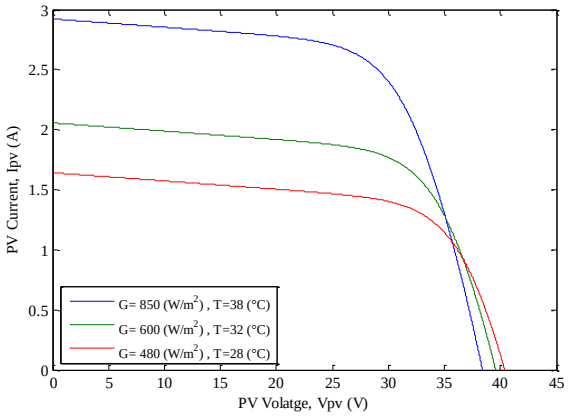

Fig.2. (I_{PV}_V_{PV}) characteristics of the PV module.

Fig.3 and Fig.4 show the PV output power (P_{PV}) for various insulations and temperatures. According to Fig.3 and Fig.4 P_{PV} will increase if insulation increase and temperature decrease and vice versa. Overall it can be said the best environmental condition for the PV module is the high solar irradiance and the low temperature.

In Fig.3 and 4, for every environmental condition there is a unique point in P_{PV} curve which is at maximum value. This maximum point needs to be tracked by the controller unit.

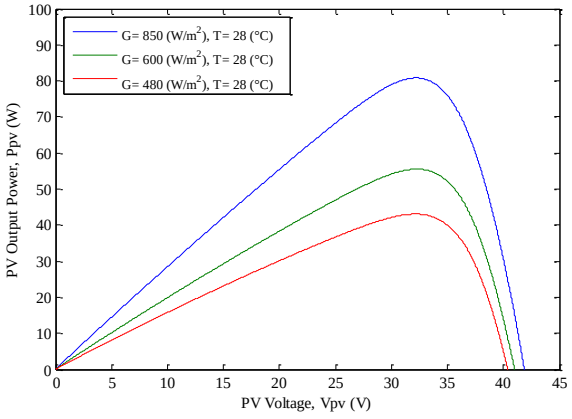

Fig.3. PV output power under different irradiances.

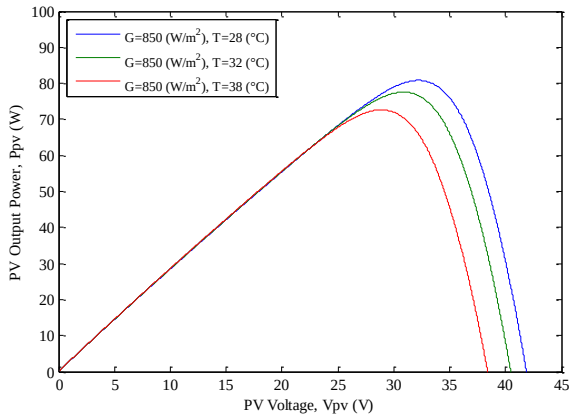

Fig.4. PV output power under different temperatures.

III. MPPT System Modeling

Fig.5 depicts the overall PV system block diagram that includes three main parts: PV module, DC/DC boost converter and MPPT unit.

Briefly, the MPPT unit measures the output power of the PV module (P_{PV}) and decides to change the duty cycle of the converter or not, accordingly.

A. DC/DC Boost Converter

The equivalent circuit model of a DC/DC boost converter is illustrated in Fig.6.

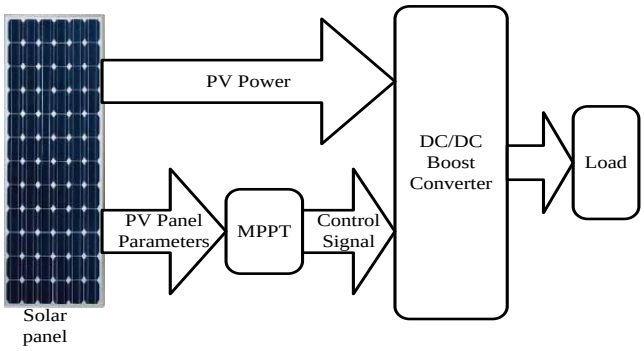

Fig.5. PV system block diagram.

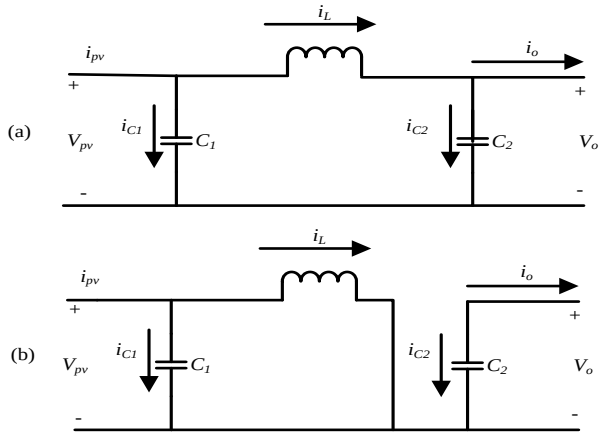

Fig.6. Equivalent circuit of a boost converter in two operation states ((a): *S*=0, (b): *S*=1).

The converter has two states of working according to the position of the switch S:

a) When the switch is off (S=0):

$$\frac{di_L}{dt} = \frac{V_{PV}(i_L)}{L} - \frac{V_o}{L} \tag{4}$$

$$\frac{dV_{PV}}{dt} = -\frac{i_L}{C_1} + \frac{i_{PV}}{C_1} \tag{5}$$

$$\frac{dV_o}{dt} = -\frac{i_L}{C_2} - \frac{V_o}{R_L \cdot C_2} \tag{6}$$

b) When the switch is on (S=1):

$$\frac{di_L}{dt} = \frac{V_{PV}(i_L)}{L} \tag{7}$$

$$\frac{dV_{PV}}{dt} = -\frac{i_L}{C_1} + \frac{i_{PV}}{C_1} \tag{8}$$

$$\frac{dV_o}{dt} = -\frac{V_o}{R_L \cdot C_2} \tag{9}$$

where V_o is the converter's output voltage, C_1 and C_2 are the capacitors, i_L and R_L are the conductance current and load respectively. Equations (4) to (9) can be combined into the one set of state equations ($S \in \{0,1\}$):

$$L\frac{di_L}{dt} = V_{PV}(i_L) - V_o \cdot (1-S) \tag{10}$$

$$C_2 \cdot \frac{dV_o}{dt} = -i_L \cdot (1-S) - \frac{V_o}{R_L} \tag{11}$$

B. Incremental Conductance Method

Because of being easily implemented, INC algorithm is used in many MPPT units [21]-[24]. The traditional INC is not capable to track maximum power point of the PV module under sudden changes in environmental conditions. INC is based on this fact that the slope of the PV output power(P_{PV}) is equal to zero at the maximum power point (12):

$$\frac{\partial P_{PV}(V_{PV}, i_{PV})}{\partial V_{PV}} = 0$$

$$\rightarrow i_{PV} + V_{PV} \cdot \frac{di_{PV}}{dV_{PV}} = 0 \rightarrow \frac{dV_{PV}}{di_{PV}} = -\frac{V_{PV}}{i_{PV}} \tag{12}$$

According to (12), when $\frac{dV_{PV}}{di_{PV}} = -\frac{V_{PV}}{i_{PV}}$ is confirmed the PV system is at its optimal power point. The flowchart of the modified INC algorithm is illustrated in Fig. 7 where *k*, *k-1* are the sampling times at *t*, *t-1* respectively.

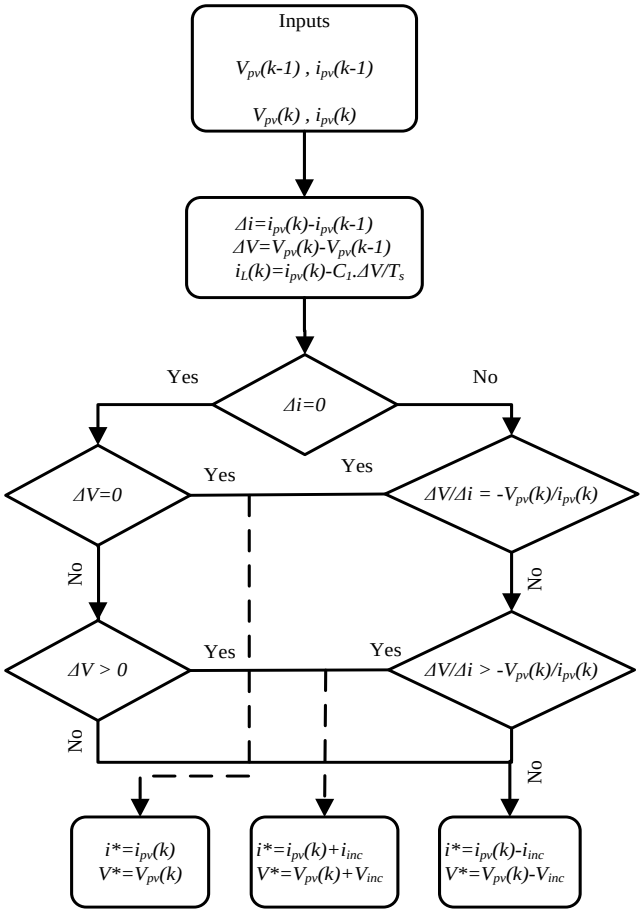

Fig.7. INC flowchart.

$i^*(k)$ is the PV output current at MPP that is defined as the increment of the PV current measurement ($i_{PV}(k)$) not as the increment of the $i^*(k)$ at previous sampling time ($i^*(k-1)$). This modification enables the system to decide and respond faster under abrupt variations in environmental conditions [25].

Equations (4) to (9) can be written in the form of the discrete time system equations considering the sampling time T_S as below:

$$i_L(k+1)=i_L(k)+\frac{T_S}{L}V_{PV}(k)-\frac{T_S}{L}V_O(k) \quad (13)$$

$$V_{PV}(k+1)=V_{PV}(k)-\frac{T_S}{C_1}i_L(k)+\frac{T_S}{C_1}i_{PV}(k) \quad (14)$$

$$V_O(k+1)=\frac{T_S}{C_2}i_L(k)+\left(1-\frac{T_S}{RC_2}\right)V_O(k) \quad (15)$$

$$i_L(k+1)=i_L(k)+\frac{T_S}{L}V_{PV}(k) \quad (16)$$

$$V_{PV}(k+1)=V_{PV}(k)-\frac{T_S}{C_1}i_L(k)+\frac{T_S}{C_1}i_{PV}(k) \quad (17)$$

$$V_O(k+1)=\left(1-\frac{T_S}{RC_2}\right)V_O(k) \quad (18)$$

According to (13) to (18), the controllable variables i_{PV} , V_{PV} can now be predicted for the next sampling time so the control actions can be obtained for the present time and the future periods, both.

C. Sliding Mode Control

Designing of the sliding mode controller consists of two states: 1. defining of the sliding surface, 2. designing of the control signal. The sliding surface is selected as the desirable values of the controllable variables and the control signal guarantees that the system states converge to the sliding surface and remain on it.

1. Designing the sliding surface:

As previously mentioned, the slope of the PV output power is zero at MPP. Therefore if we define the sliding surface as $\frac{\partial P_{PV}(V_{PV},i_{PV})}{\partial V_{PV}}=0$ the PV power will be maximized when the system state variables converge to the sliding surface [17], [18], [26].

$$\frac{\partial P_{PV}(V_{PV},i_{PV})}{\partial V_{PV}}=0$$

$$\rightarrow \frac{\partial\left(i_{PV}^2\cdot R_{PV}\right)}{\partial i_{PV}}=i_{PV}\left(2R_{PV}+i_{PV}\frac{\partial R_{PV}}{\partial i_{PV}}\right)=0 \quad (19)$$

In (19), $R_{PV}=\frac{V_{PV}}{i_{PV}}$ is the equivalent load that is connected to the PV module. The non-trivial solution of the (19) is $2R_{PV}+i_{PV}\frac{\partial R_{PV}}{\partial i_{PV}}=0$ so the sliding surface (σ) can be defined as:

$$\sigma=R_{PV}+i_{PV}\frac{\partial R_{PV}}{\partial i_{PV}} \quad (20)$$

As it can be seen in Fig.8 that determines the duty cycle of the boost converter (δ) in all operation regions, its control signal can be chosen as below:

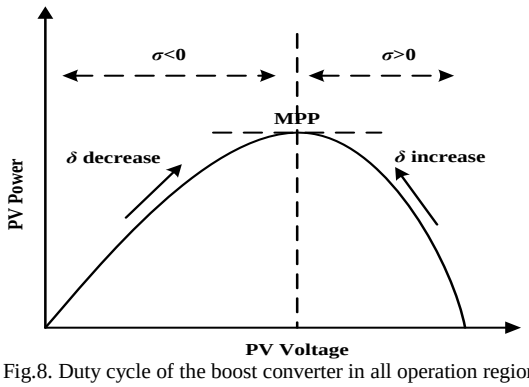

Fig.8. Duty cycle of the boost converter in all operation regions.

$$\delta_{update} = \begin{cases} \delta + \Delta\delta & \sigma > 0 \\ \delta - \Delta\delta & \sigma < 0 \end{cases} \quad (21)$$

where δ_{eq} is the equivalent control signal.

The equivalent control signal can be obtained as follow [27]:

$$\delta_{eq} = 1 - \frac{V_{PV}(i_L)}{V_o} \quad (22)$$

The duty cycle of the converter must be between 0 and 1, $0 \le \delta_{eq} \le 1$, hence the real control signal is defined as:

$$\delta = \begin{cases} 1 & \delta_{eq} + k\sigma \ge 1 \\ \delta_{eq} + k\sigma & 0 < \delta_{eq} + k\sigma < 1 \\ 0 & \delta_{eq} + k\sigma \le 0 \end{cases} \quad (23)$$

where k is a positive constant (k=0.01).

IV. Simulation Results

All simulations in this paper have been done in MATLAB/SIMULINK. In this study, Siemens SM110-24 PV panel has been selected as a PV cell. Table II summarizes the main specifications for simulations.

The solar irradiance and the temperature variations are illustrated in Fig.9. The theoretical maximum powers of the PV panel for every irradiance and temperature are tabulated in Table III.

TABLEII
MAIN SPECIFICATIONS

Parameter	Value
Inductance (L)	1.5 mH
Capacitance (C_1)	100 µF
Capacitance (C_2)	500 µF
MPPT current increment (i_{inc})	100 mA
MPPT current increment (V_{inc})	150 mV
Load (R)	50 Ω

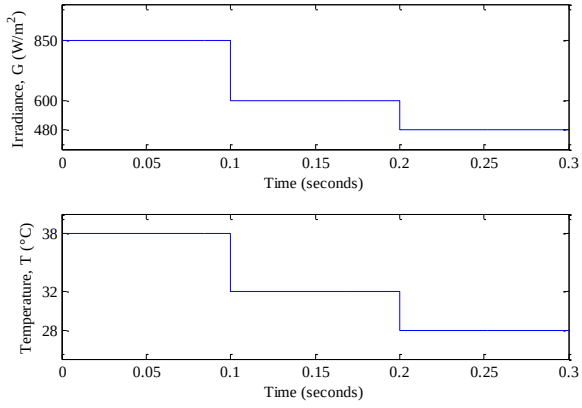

Fig.9. Simulation condition.

TABLEIII
THEORETICAL MAXIMUM POWERS

Irradiance, G (W/m^2)	Temperature, T (°C)	Theoretical Maximum Power, P_{MPP} (W)
850	38	72.64
600	32	53.39
480	28	43.07

The PV output power with SMC and INC is shown in Fig.10. The plot depicts that the both controllers can track maximum power of the PV module under environmental variations, however, the power fluctuations with SMC is much less than INC that means SMC is more robust towards the irradiance and the temperature variations.

PV extracted energy is defined as (24) in order to compare the controllers' efficiency. In Table IV, extracted PV energies for each controller are shown. The theoretical maximum PV energy during simulation is 16.909 (J).

$$\text{PV Extracted Energy} = \int_0^{0.3} P_{PV} \cdot dt \quad (24)$$

According to Table 4, sliding mode controller increases the PV system efficiency up to 5% in comparison to INC. In other words, the energy dissipation with SMC is less than INC.

If the error is defined as the difference between the PV theoretical maximum power and the PV output power ((25)), Fig.11 illustrates the error for each controller. Fig.11 verifies that SMC is more stable around MPP and the PV output power with SMC converges to MPP faster than INC while it is more precise.

$$Error = P_{MPP} - P_{PV} \quad (25)$$

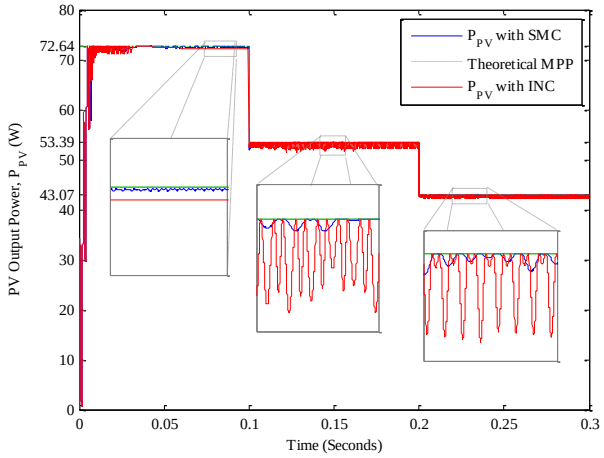

Fig.10. PV Output Power with SMC and INC.

TABLEIV
PERFORMANCE OF THE CONTROLLERS

Controller	Extracted Energy (W)	Efficiency (%)
SMC	16.6718	98.6
INC	15.8241	93.6

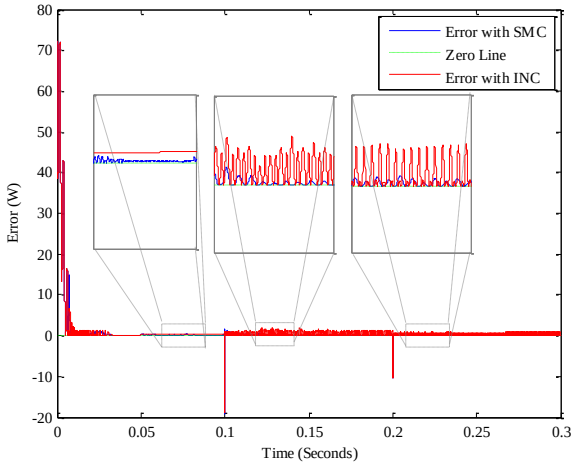

Fig.11. PV output power error with SMC and INC.

V. Conclusion

In this paper, a comparative study of sliding mode controller and incremental conductance method to track maximum power of the photovoltaic arrays provided. Simulation results indicate that both controllers can track maximum power under environmental variations. Comparing SMC with INC demonstrates that the PV output power chattering around MPP has decreased considerably using SMC therefore the PV system response is more stable. In addition SMC is faster and more precise than INC. As a result, SMC can increase the PV system efficiency up to 5% which results in less energy losses.

VI. References

[1] Z. Salameh, D. Taylor. (1990). Set-up maximum power point tracker for photovoltaic arrays, Solar Energy [Online], 44, pp. 57-61. Available: https://doi.org/10.1016/0038-092X(90)90027-A

[2] S. Lalouni, D. Rekioua, T. Rekioua, E. Matagne. (2009). Fuzzy logic control of standalone photovoltaic system with battery storage, Power Source, pp.899-907. Available: https://doi.org/10.1016/ j.jpowsour. 2009.04.016

[3] S. Zhou, L. Kang, J. Sun, G. Guo, B. Cheng, B. Cao, Y. Tang. (2010). A novel maximum power point tracking algorithms for stand-alone photovoltaic system, International Journal of Control, Automation and Systems [Online], 8 (6). pp. 1364-1371, Available: https://doi.org/ 10.1007/ s12555-010-0624-7

[4] A. Yazdani, P. P. Dash. (2009). A Control Methodology and Characterization of Dynamics for a Photovoltaic (PV) System Interfaced With a Distribution Network. IEEE Transactions on Power Delivery [Online]. 24 (3), pp.1538-1551. Available: https://doi.org/10.1109/ TPWRD.2009.2016632H

[5] E.-S. A. Ibrahim, F. F. Houssiny, H. M. Z. El-Din, M. A. El-Shibini, "Microcomputer controlled buck regulator for maximum power point tracker for DC pumping system operates from photovoltaic systems," in Fuzzy Systems Proc. Conf. [Online], Seoul, 1999, pp. 406-411. Available: https://doi.org/10.1109/FUZZY.1999.793274

[6] K. Nishioka, N. Sakitani, K. Kurobe,Y. Yamamoto, Y. Ishikawa, Y. Uraoka, T. Fuyuki. (2003). Analysis of the Temperature Characteristics in Polycrystalline Si Solar Cells Using Modified Equivalent Circuit Model. Japanese Journal of Applied Physics [Online]. 42, pp.7175-7179. Available: http://iopscience.iop.org/article/10.1143/JJAP.42. 7175/meta

[7] M. Masoum, H. Dehbonei, "Design, Construction and Testing of a Voltage-based Maximum Power Point Tracker (VMPPT) for Small Satellite Power Supply," in Small Satellite Conf. [Online], 1999. Available: https://digitalcommons.usu.edu/smallsat/1999/all1999/88/

[8] K. A. Kim, R. M. Li, P. T. Krein, "Voltage-offset resistive control for DC-DC converters in photovoltaic applications," in IEEE APE Conf. [Online], 2012, pp. 2045-2052. Available: https://doi.org/10.1109/ APEC.2012.6166103

[9] H. T. Duru. (2006). A maximum power point tracking algorithm based on $I_{mpp}=f(P_{max})$ function for matching passive and active loads to a photovoltaic generator. Solar Energy [Online]. 80 (7), pp.812-822. Available: https://doi.org/10.1016/j.solener.2005.05.016

[10] M. Veerachary. (2011). Fourth-Order Buck Converter for Maximum Power Point Tracking Applications. IEEE Transactions on Aerospace and Electronic Systems. [Online]. 47 (2), pp.893-911. Available: https://doi.org/10.1109/TAES.2011.5751233

[11] Stefan C. W. Krauter. (2006). Solar Electric Power Generation-Photovoltaic Energy Systems. (1st ed.) [Online]. Available: https://link.springer.com/book/10.1007/978-3-540-31346-5

[12] H. Al-Atrash, I. Batarseh, K. Rustom. "Statistical modeling of DSP-based Hill-climbing MPPT algorithms in noisy environments," in 20th IEEE APE Conf. [Online], Austin Texas, USA, 2005, pp. 1773-1775. Available: https://doi.org/10.1109/APEC.2005.1453286

[13] S. K. Kollimalla, M. K. Mishra. "Novel adaptive P&O MPPT algorithm for photovoltaic system considering sudden changes in weather conditions," in ICCEP Conf. [Online], Alghero, Italy, 2013, pp. 653-658. Available: https://doi.org/10.1109/ICCEP.2013.6586955

[14] L. Piegari, R. Rizzo. (2010). Adaptive perturb and observe algorithm for photovoltaic maximum power point tracking. IET Renewable Power Generation [Online]. 4(4), pp. 317-328. Available: http://dx.doi.org/ 10.1049/iet-rpg.2009.0006

[15] N. Femia, G. Petrone, G. Spagnuolo, M. Vitell. (2005). Optimization of perturb and observe maximum power point tracking method. IEEE Transactions on Power electronics [Online]. 20 (4), pp. 963-973. Available: https://doi.org/10.1109/TPEL.2005.850975

[16] A. Bidram, A. Davoudi, R. S. Balog. (2012). Control and Circuit Techniques to Mitigate Partial Shading Effects in Photovoltaic Arrays. IEEE Journal of Photovoltaics [Online]. 2(4), pp.532-546. Available: https://doi.org/10.1109/JPHOTOV.2012.2202879

[17] M. R. Mojallizadeh, M. A. Badamchizadeh, S. Khanmohammadi, M. Sabahi. (2016). Designing a new robust sliding mode controller for maximum power point tracking of photovoltaic arrays. Solar Energy [Online]. 132, pp. 538-546. Available: https://doi.org/10.1016/ j.solener.2016.03.038

[18] D. Rekioua, A. Y. Achour, T. Rekioua. (2013). Tracking power photovoltaic system with sliding mode control strategy. Energy Procedia [Online]. 36, pp.219-230. Available: https://doi.org/ 10.1016/j.egypro.2013.07.025

[19] Altas, I., Sharaf. (2008). A. A novel maximum power fuzzy logic controller for photovoltaic solar energy systems. Renewable energy [Online], 33(3), 388-399. Available: https://doi.org/10.1016/j.renene. 2007. 03.002

[20] Masoum, M., Sarvi. , (2005). M. A new fuzzy-based maximum power point tracker for photovoltaic applications. Iranian Journal of Electrical and Electronic Engineering [Online], 1(1), 28-35. Available: http:// www. sid.ir/En/Journal/ViewPaper.aspx?ID=127814

[21] H. De Battista, R. J. Mantz. (2002). Variable structural control of a photovoltaic energy converter. IEE Proceeding- Control Theory and Applications [Online]. 149 (4), pp. 303-310. Available: http://dx.doi.org/10.1049/ip-cta:20020556

[22] I. Houssamo, F. Locment, M. Sechilariu. (2010). Maximum power point tracking for photovoltaic power system: Development and experimental comparison of two algorithms. Renewable Energy [Online]. 35 (10), pp. 2381-2387. Available: https://doi.org/10.1016/j.renene.2010.04.006

[23] M.A.S. Masoum, H. Dehbonei, E.F. Fuchs. (2002). Theoretical and experimental analyses of photovoltaic systems with voltage and current-based maximum power point tracking. IEEE Transactions on Energy Conversion [Online]. 17 (4), pp. 514-522. Available: https://doi.org/10.1109/TEC.2002.805205

[24] R. Rajesh, M. C. Mabel. (2015). A comprehensive review of photovoltaic systems. Renewable and Sustainable Energy Reviews [Online]. 51, pp. 231-248. Available: https://doi.org/10.1016/ j.rser.2015.06.006

[25] P. E. Kakosimos, A. G. kladas. (2011). Implementation of photovoltaic array MPPT through fixed step predictive control technique. Renewable Technique [Online]. 63 (9), pp. 2508-2514. Available: https://doi.org/ 10.1016/j.renene.2011.02.021

[26] M. B. Shadmand, M. Mosa, R. S. Balog, H. Abu Rub. "An improved MPPT technique for high gain DC-DC converter using model predictive control for photovoltaic applications," in IEEE APE Conf. Fort worth Texas, USA, 2014. Available: https://doi.org/10.1109/APEC.2014.6803730

[27] Slotine, J.-J. E, Li, W. (1991).“ Applied nonlinear control”(Vol. 199, Vol. 1): Prentice hall Englewood Cliffs, NJ. Available: https://s3.amazonaws.com/academia.edu.documents/33582713/Applied_Nonlinear_Control_Slotine.pdf?AWSAccessKeyId=AKIAIWOWYYGZ2Y53UL3A&Expires=1517482041&Signature=08tx4djAx6YUwX5bXEOOvIIpinU%3D&response-content-disposition = inline %3B%20filename%3DSlotine_at_BULLET_Li_APPLIED_NONLINEAR_C.pdf

VII. BIOGRAPHY

Babak Mehdizadeh Gavgani has born in Tabriz, Iran on August 31, 1991. He received his B.Sc. in Control Engineering from university of Tabriz in 2014. In 2015 he started his M.Sc. in Control Engineering at Seraj University in Tabriz and he finished it in 2017.

His research interests include optimization and control of renewable energy (solar and wind) systems and their applications.